Cavity quantum electrodynamics with quantum dots in microcavities

Bakker, M.P.

Chapter 1

Introduction

In this introductory chapter, we will motivate our work and discuss future applications of cavity quantum electrodynamics (QED). We will also provide a theoretical description of cavity QED, including the important concepts of dressed states and avoided crossing. Next, we will compare various cavity QED systems, first the non-semiconductor based systems and then various semiconductor cavity architectures, and motivate the choice for our system. We conclude with an overview of the chapters in this thesis and the relationship between them.

1.1 Towards deterministic spin–photon entanglement

As a general motivation for the work presented in this thesis, we will present a scheme on how to generate deterministic spin–photon entanglement using cavity quantum electrodynamics (QED). In this thesis significant progress will be presented towards realizing this experiment, which could form the basis of much future research and several novel applications.

Cavity QED deals with the interaction between light confined in a cavity, and a single atom or other emitter. One manifestation is that a transmittive cavity can be turned into a reflective one by coupling a single atomic dipole transition to it [1–3]. We aim to use this property to create entanglement between light and matter.

Figure 1.1 shows the generic geometry of a cavity together with an atom that has two ground states that couple to dipole transitions of different energy and/or polarization. These two states can be for example the hyperfine split states of an atom, or the Zeeman split spin states of a singly charged quantum dot (QD). We want to realize the latter and will thus refer to these ground states as the spin up $|\uparrow\rangle$ and spin down $|\downarrow\rangle$ states. Depending on the spin state, the incoming photon will couple to an optical transition or not, and subsequently will be reflected or transmitted. If the atom is now prepared in a superposition state $|\Psi\rangle_{atom} = \alpha\,|\uparrow\rangle + \beta\,|\downarrow\rangle$ with $|\alpha|^2 + |\beta|^2 = 1$, the cavity mediated interaction results in an entangled output state $|\Psi\rangle_{out}$ between the photon and the atom:

$$|\Psi\rangle_{in} = |\phi\rangle_{photon} \otimes |\Psi\rangle_{atom} \quad \rightarrow \quad |\Psi\rangle_{out} = \alpha\,|R,\uparrow\rangle + \beta\,|T,\downarrow\rangle\,, \tag{1.1}$$

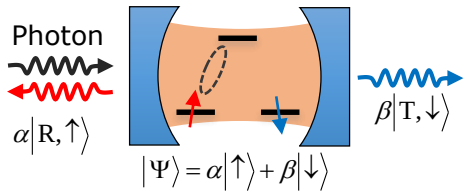

Figure 1.1: Scheme for the creation of deterministic spin–photon entanglement. The atom (or QD) is prepared in a superposition of two ground states, which for a QD are the spin up/down states of a confined single-charge. An incident photon, with a frequency and polarization that only couples to one of the two transitions, is subsequently reflected and transmitted depending on the spin state. This operation creates entanglement between the spin state and the spatial degree of freedom of the photon.

where $|\phi\rangle_{photon}$ denotes the photon being initially in the input port, and $|R/T\rangle$ denotes the photon being in the reflection/transmission mode. This process thus creates deterministic spin-photon entanglement. The entanglement protocol can be verified by interfering, for example, the two possible photon paths on a beamsplitter; the output port of the photon will then depend on the value of α and β.

Light-matter entanglement has been realized using atoms [4], and solid–state spin systems such as NV-centers [5] and QDs [6, 7]. In these systems the (artificial) atom is first excited and then relaxes to one of the two spin–split ground states. As these ground states are typically non-degenerate the polarization as well as the frequency of the emitted photon becomes entangled with the ground-state spin. This implies that either the polarization or the frequency information of the photon needs to be 'erased' in order to eliminate the 'which-path' information, and this postselection operation limits the success probability. Postselection on spontaneously emitted photons can be used to entangle two qubits at a distance [8, 9], but as these protocols are of a probabilistic nature many experiments need to be performed in order to select the desired outcome. Nevertheless, experiments have been demonstrated that remotely entangle two atoms [10], two NV-centers [11], or even teleport a quantum state [12]. A deterministic protocol however, as the one we describe here, will increase the success rate and is especially favorable, if needed, for further scaling up to multipartite entangled qubit systems.

The work presented in this thesis has a dual motivation. On the one hand, it is driven by curiosity whether the intriguing effects predicted by quantum mechanics can be realized in a (solid-state) system in the lab. These experiments can form a fundamental test of textbook physics on the interaction between atoms and single light quanta, and non-local quantum entanglement.

On the other hand, our system shows promise for new applications and technologies based on the principles of quantum mechanics. We will discuss these applications in the next session.

1.2 Applications of cavity QED

Various applications of cavity QED can be envisioned, which motivates many research groups both inside and outside of academia to work in this interesting field. In the following we will mention some applications, even though some may seem to lie far ahead in the future.

1.2.1 Quantum information applications

Many quantum information processing (QIP) applications can be realized that rely on (deterministic) spin-photon entanglement. Schemes to entangle a single spin with a single photon can be extended to entangle multiple spins, and to form a quantum network [13, 14]. Such a quantum network would consist of spins in cavities where quantum states are stored and manipulated, which are connected by optical channels that distribute quantum information.

A quantum network enables to perform cluster state quantum computing [9, 15, 16]. The creation of deterministic entanglement can also be used to realize a quantum repeater, which is essential to deal with losses in long-distance transport of quantum information via photons possible [8, 17, 18]. Finally, it could be used for quantum metrology [19], and for example enhance the sensitivity of gravitational wave detectors [20]

1.2.2 Non-classical light sources

A cavity QED system can be used to generate non-classical states of light, which could realize a whole range of technologies that make use of the quantum mechanical properties of photons [21]. Quantum cryptography can for example be realized with single-photon [22], or entangled-photon sources [23]. See for a review Ref. [24]. Single-photon sources and detectors, and linear optical networks can make photonic linear quantum computation possible [25]. A recent proposal describes how a cavity quantum electrodynamics scheme can in principle be used to realize an emitter of so-called N-photon bundles [26]. These could be used to create so-called NOON states [27], and for quantum lithography and metrology [28].

A cavity with an emitter coupled to it can ensure the efficient generation and collection of such (quantum) light. For practical applications an electrically driven room temperature cavity QED system would be ideal, but has not yet been realized. Significant progress has been realized with semiconductor QD systems, albeit limited to cryogenic temperatures. Some examples include

an electrically driven single-photon source with QDs in a p-i-n junction [29], electrically driven single-photon emission from a QD-micropillar system [30], optically pumped emission of entangled photon pairs through the biexciton decay of a neutral QD [31], and an ultrabright source of entangled photon pairs using a bimodal photonic molecule consisting of two coupled microcavities [32].

1.2.3 Optical interconnects

Optical interconnects aim to combine electronics and photonics in the same device. They are of great interest, among others because the high frequency transfer of signals is much more energy consuming for electrical signals compared to optical signals [33, 34]. Converting an electrical signal into an optical signal, and vice versa, relies on strong light-matter interactions. For this purpose cavity QED could be of interest, as it enables optical non-linearities at small photon numbers. Large-scale applications probably require a room temperature on-chip system, most likely one that is compatible with the current industry standard of Silicon photonics technology.

1.3 Theory of cavity quantum electrodynamics

The research field of cavity QED deals with the interaction between light confined in a cavity and matter, typically in the form of atoms or 'artificial' atoms like quantum dots. In section 1.3.1, we will first introduce the semiclassical approach for an atom in a cavity, a description that perfectly suffices throughout most of this thesis. In section 1.3.2, we will discuss the Jaynes-Cummings model, which incorporates the quantum nature of photons and the atom/emitter. Two important concepts of this model are the occurrence of dressed states and the avoided crossing. We will introduce these in section 1.3.3 and show how they appear in our measurement results.

1.3.1 Semiclassical approach of a two-level atom in a cavity

A schematic picture of a two-level atom in a Fabry-Perot type cavity is shown in Fig. 1.2. The cavity has an in-coupling efficiency η, equal mirrors with an intensity loss rate κ_m through each mirror, and an absorption/scattering loss rate κ_s. The two level atom is introduced as a dielectric medium with a normalized electric susceptibility proportional to $2C/(1-i\Delta')$, where $\Delta' = (\omega - \omega_a)/\gamma$ is the difference between the laser and the atom angular frequency relative to the atom dephasing rate γ. The cooperativity C can be intuitively seen as the ratio between the atom absorption rate, and a function of the total absorption and loss rate of the cavity. Following the standard approach of calculating the transmission amplitude of a Fabry-Perot

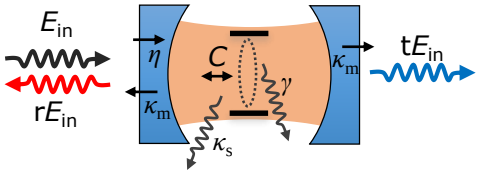

Figure 1.2: Schematic picture of a two-level atom in a cavity. An incoming photon with electric field strength E_{in} is reflected and transmitted with relative amplitudes r and t, respectively. The cavity has an incoupling efficiency η, mirrors with equal loss rates κ_m and an internal loss rate κ_s. The two-level system has a cooperativity C and a dephasing rate γ.

cavity with a dielectric medium, we find:

$$t = \eta \frac{1}{1 - i\Delta + \frac{2C}{1-i\Delta'}}, \tag{1.2}$$

where $\Delta = 2(\omega - \omega_c)/\kappa$ is the difference between the laser and cavity angular frequencies divided by the total cavity decay rate $\kappa = 2\kappa_m + \kappa_s$. The total transmission is now given by $T = |t|^2$ and the reflectivity is given by $R = |1 - t|^2$.

This model describes the time-averaged optical properties of the system in the low intensity limit (less than 1 photon per cavity lifetime), where no single emitter/absorber effects play a role. It can be easily expanded for multi-level atomic systems with different polarized transitions, as will be described in Ch. 6.

1.3.2 Jaynes-Cummings model

The Jaynes-Cummings model was introduced in 1963 by Edwin Jaynes and Fred Cummings [35]. Neglecting the vacuum energy and losses, and applying the rotating wave approximation, they described the Hamiltonian of a two-level atom coupled to a cavity by:

$$\begin{aligned} H &= H_{field} + H_{atom} + H_{interaction} \\ &= \hbar\omega_c a^\dagger a + \hbar\omega_a \sigma_z^\dagger \sigma_z + \hbar g(a^\dagger \sigma_- + \sigma_+ a), \end{aligned} \tag{1.3}$$

where $a(a^\dagger)$ and $\sigma_-(\sigma_+)$ are lowering (raising) operators of the optical field and atom, respectively. The coupling strength g between the cavity and atom is given by: $g = g_0\sqrt{n+1}$, where n are the number of photons in the cavity and $g_0 = \sqrt{C\kappa\gamma}$. The case $n = 0$ corresponds to the situation where the system contains one excitation, either in the cavity or in the atom.

We now consider a single excitation of the system in the case where the cavity and atom are resonant $\omega = \omega_c = \omega_a$ and no losses of the system are taken

into account yet. For the uncoupled case ($g_0 = 0$), the system can be described by the degenerate energy eigenstates $|\Psi_+\rangle = |e\rangle\,|n\rangle$ and $|\Psi_-\rangle = |g\rangle\,|n+1\rangle$ that describe either an excitation in the cavity field or in the atom. Here $|g\rangle$ and $|e\rangle$ denote the atom being in the ground and excited state, respectively, and $|n\rangle$ denotes the number of photons in the cavity. However, when the system is coupled, the eigenstates $|\Psi_\pm\rangle$ with eigenenergies $E^n_\pm$ are given by:

$$|\Psi_\pm\rangle = \frac{1}{\sqrt{2}}(|e,n\rangle \pm |g,n+1\rangle), \qquad E^n_\pm = (n+1)\hbar\omega \pm \hbar g_0\sqrt{n+1}. \tag{1.4}$$

These so-called dressed states contain simultaneously an excitation in the optical field and in the atom. The phenomenon that the bare states are split into dressed states with energy splittings $\Delta E^n = E^n_+ - E^n_- = 2\hbar g_0\sqrt{n+1}$, is referred to as the Jaynes-Cummings ladder. When the detuning between the cavity and atom is gradually decreased, a gradual transition from bare states, which would cross in energy at zero detuning, to dressed states, which are split in energy, occurs. In the next session we will demonstrate how this avoided crossing appears in our system.

In order to take losses into account, the system can be generically described using the Heisenberg picture, where the equation of motion of any operator Θ becomes:

$$\frac{d\Theta}{dt} = -\frac{i}{\hbar}[\Theta, H] + L(\Theta). \tag{1.5}$$

Here $L(\Theta)$ is the Markovian loss operator. The loss rates of the cavity and atom can again be introduced as κ and γ. The solution of the energy eigenstates $E^n_\pm$ of the coupled system, with angular frequency $\omega^n_\pm$ and dephasing rate $\Gamma^n_\pm$, is given by:

$$E^n_\pm = \hbar\omega^n_\pm - i\Gamma^n_\pm = \frac{1}{2}((2n+1)\hbar\omega_c + \hbar\omega_a) - \frac{i}{2}((2n+1)\kappa + \gamma) \pm\sqrt{(n+1)g^2 + \frac{1}{4}[(\hbar\omega_c - \hbar\omega_a) - i(\kappa-\gamma)]^2}. \tag{1.6}$$

This equation shows that in the low excitation intensity limit $n = 0$ for $g > \gamma, \kappa$ and $\omega_c = \omega_a$, the dephasing rate Γ becomes approximately equal to the average of κ and γ, which demonstrates the mixing of the cavity and atom character for the dressed states. For $n > 0$ the bare states contain either $n+1$ photons in the cavity, and the total decay rate equals $(n+1)\kappa$, or the bare state contains n photons in the cavity and one excitation of the atom, and the decay rate equals $n\kappa + \gamma$. Subsequently, for $g > \gamma, \kappa$ the dephasing rate of the dressed states are approximately the average of these decay rates $\Gamma \approx \frac{1}{2}((2n+1)\kappa+\gamma)$

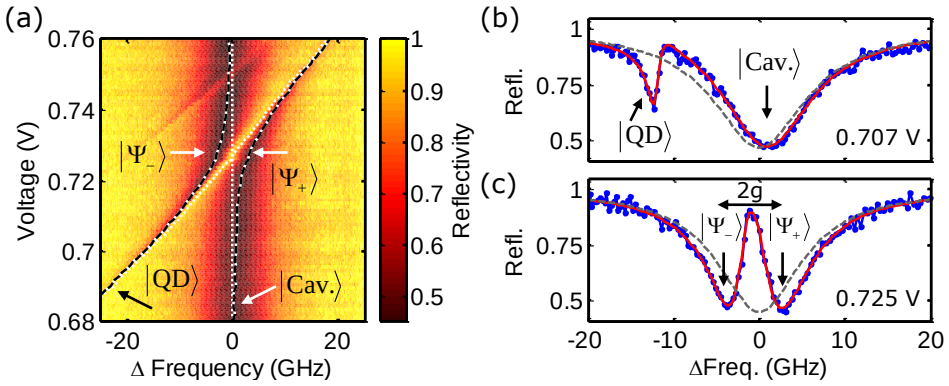

Figure 1.3: Signatures of dressed states and avoided crossing. (a) shows a reflectivity color map as function of the frequency detuning of a laser, scanned across the QD-cavity system, and the bias voltage. White dashed lines are QD and cavity frequencies, black-white lines are the frequencies of the two dressed states. (b,c): cross-sections of the reflectivity scans when the QD is detuned (b) and when the QD is in resonance (c). Grey dashed lines show the empty cavity resonance.

Finally, the input-output formalism can be used to calculate the reflection and transmission [36–39]. In the low excitation intensity limit, this yields the same results as for the semiclassical model. For larger excitation intensities calculating the reflectivity and transmittivity spectrum becomes non-trivial as the input state is a superposition of Fock states, and numerical methods such as provided by the Quantum Optics toolbox can be used [40].

In the literature two regimes are typically defined:

- Intermediate coupling regime, also called weak coupling or Purcell regime. This regime is defined as $\kappa > g > \gamma$. The Purcell effect, the enhancement of the spontaneous emission rate, is associated with this regime.
- Strong coupling regime, for $g > \gamma, \kappa$. Coherent oscillations of the cavity and atom excitation take place before light leaks out of the cavity.

1.3.3 Dressed states and avoided crossing

In this subsection we will demonstrate how dressed states and the avoided crossing are visible in our measurements. Low intensity ($P_{in} = 1$ pW) reflectivity measurements, such that the system contains maximally one excitation ($n = 0$), are presented in Fig. 1.3. In these scans a QD transition is tuned through the (stationary) cavity resonance, as function of applied bias voltage through the DC Stark effect. A low reflectivity corresponds with the laser

being resonant with an optical transition, either from the cavity, the QD, or the dressed state. The white dashed lines in Fig. 1.3 (a) represent the QD and cavity resonance frequencies, and black-white dashed lines, which nicely follow the reflectivity minima, represent the frequencies of the dressed states.

When the QD and cavity resonances are detuned from one another, as is the case in Fig. 1.3 (b), the QD is characterized by a much narrower transition compared to the broad cavity resonance, since $\gamma \ll \kappa$. When the QD is now tuned towards the cavity resonance, an avoided crossing is visible in Fig. 1.3 (a) and the eigenstates are now the dressed states $|\Psi_-\rangle$ and $|\Psi_+\rangle$. Figure 1.3 (c) shows the reflectivity spectrum when the QD is tuned at the exact cavity resonance. The dressed states are now visible as resonances that have FWHMs that are the average of the FWHM of the QD and the cavity resonance; this clearly indicates the mixed character of these states. Since the splitting $2g/2\pi$ between the two states is larger than the $(2\gamma/2\pi)$ FWHM of the QD resonance, but is smaller than the $(\kappa/2\pi)$ FWHM of the cavity resonance, $\kappa > g > \gamma$ and the system is in the intermediate coupling regime.

1.4 Non-semiconductor cavity QED systems

In this section we will briefly introduce three cavity QED systems: (i) atoms in cavities, which historically were first studied, (ii) atoms in nanophotonic structures, which in recent years follows up on the previous system, and (iii) superconducting circuit QED, which is one approach for realizing cavity QED in the solid-state. In the next session we will continue with a description of the other solid-state approach, semiconductor based systems, which includes our system.

Atoms in cavities

A system with an atom in a cavity has been realized with microwave and optical cavities. Two examples are shown in Figure 1.4 (a,b). Atoms are placed in a Fabry-Perot cavity either by applying a transient flux of atoms, as is the case in the two examples, or by using an optical trap.

These systems enabled for the first time cavity QED and lots of other new physics to be explored. One early investigated manifestation is the change of the spontaneous emission rate of atoms; it can be accelerated when placed in a resonant cavity [49, 50], or it can be suppressed [51], depending on whether the local density of states is increased or decreased, respectively. A review of early work (already from the 80s) is provided by Ref. [52]. The experiments were extended to other ground-breaking work such as the non-destructive manipulation of single-atoms with photons (Wineland, [53]), and the manipulation of single-photons with atoms (Haroche, [54]). This and other work led

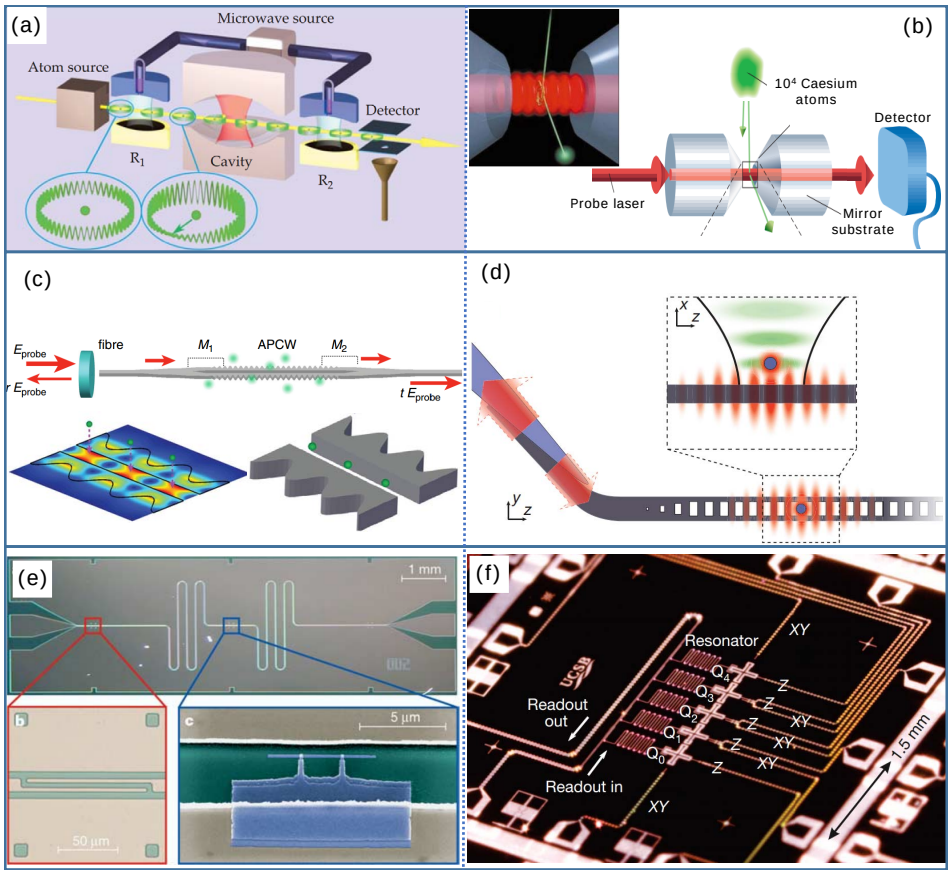

Figure 1.4: Examples of various non-semiconductor cavity QED systems. (a) Schematic illustration of atoms that are sent through a microwave cavity [41] and (b) an optical cavity [42, 43] (modified image). (c) Schematic image of atoms (green dots) in a fiber-coupled 'alligator' photonic crystal waveguide (APCW) [44]. (bottom-left) shows finite-element-method simulation of the guided mode electric field magnitude [45]. (d) Schematic drawing of a single-atom trapped in the evanescent field from a one-dimensional photonic crystal that is attached to a tapered optical fibre [46]. The inset shows the trapping lattice (green), formed by the interference of a set of optical tweezers and its reflection from the photonic crystal. (e) Electron microscope images of coplanar waveguide resonator (top) with capacitive couplers (bottom-left) to feed lines and (bottom-right) a Cooper pair box, which were used for the first circuit QED demonstration [47]. (f) Optical image of a device with 5 transmon qubits (Q_0-Q_4) coupled via nearest-neighbour coupling, controlled using the microwave/DC lines XY/Z, and read-out using resonators [48].

to the 2012 Noble prize being awarded to S. Haroche and D. Wineland "for ground-breaking experimental methods that enable measuring and manipulation of individual quantum systems". Other research highlights up to now include among others the realization of strong coupling with a single-atom in an optical cavity [55], demonstration of a quantum phase gate [56], and the demonstration of the photon blockade effect [1] by the Kimble group, and recent work in the Rempe-Ritter group, such as the realization of a single-atom quantum memory [57], the nondestructive detection of an optical photon [58], and a quantum gate between a flying optical photon and a single trapped atom [59].

In general, atoms are well suitable for quantum information applications as they are naturally identical and highly coherent, even though coherence times are typically limited to values on the order of ∼200 ms [60] due to electric or magnetic field = variations in the environment of the trapped atom. However, large and complex setups are required, for example combining complicated atom trap and optical cooling techniques. This is a major challenge for scaling these experiments further up to many distant qubit networks.

Atoms in nanophotonic structures

An interesting approach towards on-chip atom-photon manipulation is provided by trapping atoms in nanophotonic structures. Several systems have been realized, see Fig. 1.4 (c,d), such as an atom trapped in the evanescent field of a tapered optical nanofibre [61], an atom trapped in the guided mode of a double-beam photonic crystal waveguide [44, 45], and an atom trapped using an optical tweezer near a photonic structure [46, 62]. Some research highlights up to now include the realization of a quantum phase switch [46] and the all-optical routing of single photons by a one-atom switch controlled by a single-photon [63]. It is an emerging technology and promises many more great results in the near future.

Superconducting circuit QED

Superconducting circuits are one of the most promising candidates to form a qubit in a future quantum computer, as they combine on-chip integrability and scalability, electronic control, and ever increasing coherence times (see for a review [64–66]). Coupling these circuits to microwave photons confined to a resonator has proven to form an excellent platform for cavity (also called circuit) QED experiments. Figure 1.4 (e) shows the first system with which strong coupling was achieved. In a future quantum computer architecture, resonators will most likely have an important role, either to read-out individual qubits, or to create entanglement between separate qubits in the same

cavity [67]. A state-of-the-art system with 5 neighbouring qubits is shown in Fig. 1.4 (f). A drawback of superconducting circuits is that they require a working temperature of typically < 100 mK, and < 100 GHz qubit frequencies, which therefore restricts the system to microwave photons which require relative large system dimensions (many mm's).

1.5 Semiconductor cavity QED systems

Semiconductor systems are an attractive candidate for cavity QED as they promise scalability an on-chip integration. In this section, we will first mention some advantages and some of the main challenges. Next, we will present an overview of various cavity architectures. Based on the requirements for applications in quantum information processing, we will discuss the advantages and disadvantages of the several systems, and motivate the choice for our own particular system.

1.5.1 Advantages of semiconductor based cavity QED systems

A major motivation to work with semiconductor systems is that the semiconductor industry offers a well-developed 'toolbox' for nanophotonics, which promises scalable and on-chip integrated systems. Furthermore, compared to for example superconducting circuits, systems can be realized at optical frequencies. This offers a promise to be integrated with existing optical fiber communication technology, but it is also practical to work at optical frequencies in a lab.

Challenges

In order to enable quantum information processing applications, a semiconductor cavity QED system has to be realized with on the one hand coherent, identical qubits, and on the other hand a cavity that enables access to the intermediate or strong coupling regime, and a high in- and out-coupling efficiency. This has remained a major challenge for the various types of semiconductor systems, especially the necessity to combine these two requirements.

Qubits realized in III-V semiconductor materials, such as the InAs quantum dots in an $Al_xGa_{1-x}As$ structure which are the main topic in this thesis, have the disadvantage that they suffer from fast <10 μs decoherence due to coupling with nuclear spins and only operate at cryogenic temperatures due to coupling with phonons (see for various reviews for example [68–71]). The decoherence rate might seem fast, but picosecond coherent optical manipulation rates still enable many operations to be performed [72–74], and also 4 K cryogenic temperatures are nowadays easily accessible with many commercial cryostat systems. Various cavity architectures suitable for cavity QED can be

realized in III-V semiconductor material, as we will discuss in the next session.

Qubits have also been realized in various other nuclear spin-free semiconductor materials that do show long coherence times, even at room temperature. Room temperature coherence times have been reported of 40 μs for defect spins in SiC [75], more than 1 s for the nuclear spin of an ^{13}C atom coupled to an NV-centers in diamond [76], and even more than 39 minutes for ionized P donors in purified ^{28}Si [77]. Fabrication of cavities and scalable architectures in these materials offers great future promise, but has yet to be demonstrated for these highly coherent qubits.

1.5.2 Overview of semiconductor cavity architectures

Several semiconductor cavity architectures have been realized, of which several examples are shown in Fig. 1.5. We focus here on cavity systems realized with III-V semiconductor material ($Al_xGa_{1-x}As$) in which InAs self-assembled QDs are embedded, but some cavity architectures are also applicable for other materials. As every system has its advantages and disadvantages, we will compare them based on the requirements necessary for quantum information applications, which are:

- Charge control by externally applied potential in order to use singly charged QDs.
- Access to the intermediate or strong-coupling regime.
- Good cavity in- and out-coupling efficiencies.

Additionally, some system parameters that are not strictly crucial, but would still be of great benefit:

- Polarization degenerate cavity modes, to utilize the polarization degree of freedom of photons next to the spatial and frequency degree of freedom.
- Spatial and spectral alignment possibility, and/or the possibility to tune cavity or QD properties.

We will briefly introduce the various cavity designs and discuss these criteria.

(a) Photonic crystal cavities

Photonic crystal cavities consist of a defect in a 2D photonic crystal lattice, which is typically a $\lambda/2$ thick slab perforated with holes and underetched by removing a sacrificial layer. Light is typically confined to an extremely small volume $V < \lambda^3$, while still allowing reasonably high Q-factors of $\sim 10^4$. The top of Fig. 1.5 (a) shows an example of an H1 cavity (1 hole missing in a

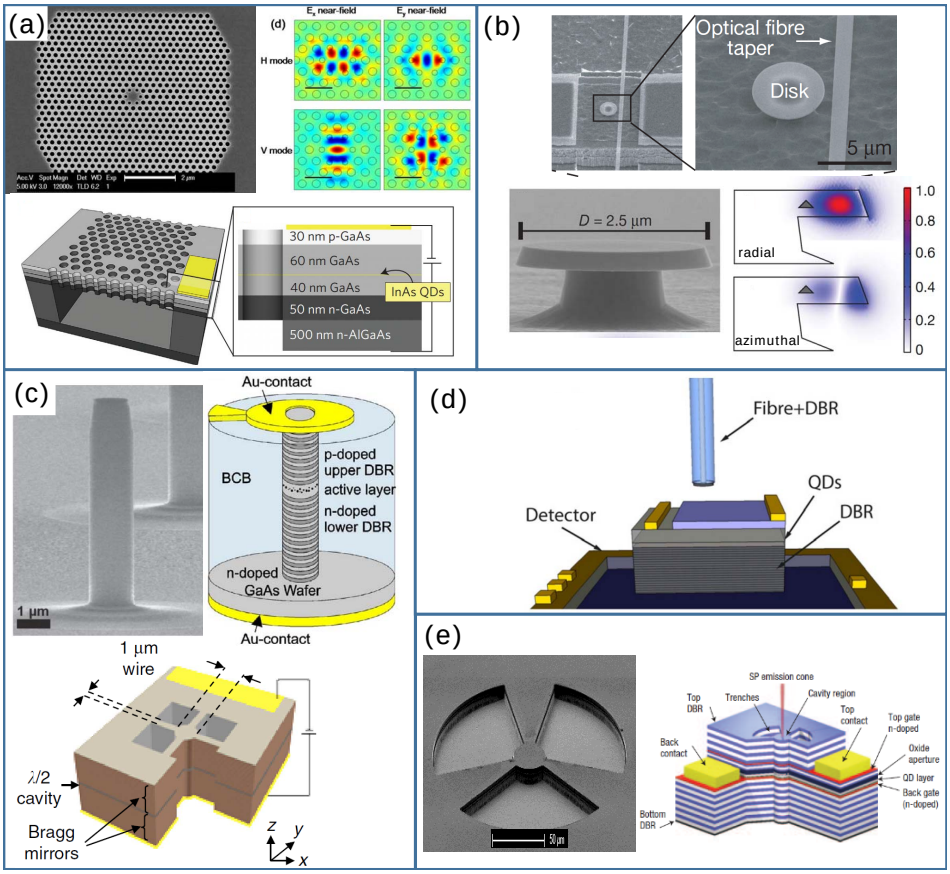

Figure 1.5: Various semiconductor cavity QED systems. (a) *Photonic crystal cavities*: (top-left) SEM image of far-field optimized H1 cavity, (top-right) FDTD simulated near-field electric field amplitudes [78], (bottom) illustration and layer thicknesses of an electrically contacted L3-type cavity [79]. (b) *Microdisk cavities*: SEM images of a microdisk coupled to a tapered fiber, and (bottom-right) finite-element-method simulations of the radial and azimuthal electric field components. (c) *Micropillar cavities*: SEM image of a freestanding MP (top-left) [80], and schematic images of electrically controlled MPs (top-right) [81] and (bottom) [82]. (d) *Combined fiber-tip and DBR Fabry-Perot cavity*, schematically shown [83]. (e) *Oxide-aperture micropillar cavity* (this thesis): (left) SEM image and (right) schematic drawing.

hexagonal lattice), of which the collection efficiency of the far-field has been optimized [78]. The bottom of Fig. 1.5 (a) shows an electrically contacted L3 cavity (3 missing holes in a row), which was used to study a single QD spin [79]. Properties of photonic crystal cavities are:

- Voltage contacts can be incorporated [79, 84].
- Strong coupling regime has been realized [85].
- The in- and out-coupling to external fields is typically poor (1-10%). On-chip coupling to waveguides is possible with near-unity efficiency [86].
- Polarization degeneracy is challenging to obtain, but can be done with AFM nano-oxidation [87].
- Deterministic spectral and spatial matching is possible [88][89]. In situ QD–cavity tuning can be performed by, among other techniques, temperature tuning [85], gas adsorption [88], and strain tuning [90].

(b) Microdisk resonator

A microdisk resonator as shown in Fig. 1.5 (b) consists of an etched torus that balances on a central post. First a mesa-type structure is produced through electron beam lithography and plasma dry etching, which is followed by a wet undercut etching step. Due to total internal reflection, a whispering gallery mode exists in the microresonator, which typically has a large $V \sim 100\lambda^3$ mode volume and very large Q-factor $Q \sim 10^6$. Coupling to external fields can be (in principle ideally) done via nearby waveguides, for example in the form of a tapered fiber. Advantages and disadvantages of microdisk resonators are:

- Voltage contacts are not possible.
- Strong coupling regime has been realized [3].
- In- and out-coupling can be performed on-chip to tapered fibers.
- Polarization control is not possible.
- Cavity tuning is possible for example through gas adsorption.

(c) Freestanding micropillar

Freestanding micropillars (MPs) consist of two distributed Bragg reflectors (DBRs) made from GaAs and $Al_xGa_{1-x}As$ (typically $x = 0.90$) that embed a λ-thick GaAs region containing QDs. A circular MP is then etched to define the transverse mode confinement. The top–left corner of Fig. 1.5 (c)

shows an example of a freestanding MP [80], which was used to demonstrate photon antibunching in the strong coupling regime. The other two figures show examples of electrically contacted MPs [81, 82]. Characteristics of micropillar devices are:

- Voltage contacts are challenging to realize [81, 82], and a deterministically singly–charged QD has yet to be realized.
- Strong coupling regime has been realized [91].
- In- and out-coupling to external fields is excellent.
- Polarization degeneracy can be achieved by controlling the micropillar shape with great accuracy [32].
- Deterministic spectral and spatial matching is possible [92]. Tuning can be performed by varying the temperature.

(d) DBR and fiber tip cavities

Figure 1.5 (d) shows a Fabry-Perot cavity consisting of a bottom DBR with a layer containing QDs on top of it, and a fiber tip on which a concave DBR has been coated. The spatial position of the cavity, and the length of the cavity (and thereby its resonance) are controlled by tuning the fiber tip position [83]. This cavity configuration holds promise to also realize strongly coupled system with materials that are not easily processed, for example NV-centers in diamond [93]. A major challenge is however the sub-nm mechanical stability that is required. Properties of DBR and fiber tip cavities are:

- Voltage contacts can be incorporated.
- Intermediate coupling regime has been achieved.
- In- and out-coupling efficiency can in principle be near-unity.
- Polarization degeneracy is limited by birefringence and non-perfect concave etching of the fiber tip.
- Deterministic spectral and spatial matching is possible.

(e) Oxide apertured micropillars

These cavities are the main subject of this thesis, and are depicted in Fig. 1.5 (e). The structure consists of two DBRs that embed a λ thick GaAs layer containing QDs in the center. Transverse mode confinement is provided by an oxide aperture, where the the large refractive index difference between the oxide ($n_{ox} \approx 1.5$) and unoxidized AlAs ($n_{AlAs} \approx 2.9$) leads to confinement in the unoxidized center of the micropillar.

We believe the oxide-apertured system is an excellent platform for QIP applications:

- Voltage contacts can be incorporated.
- Intermediate coupling regime achieved. Access to the strong coupling regime is partly limited by the relatively large mode volume (typically $\sim 10\lambda^3$).
- In- and out-coupling efficiencies can in principle be near-unity.
- Polarization degeneracy can be obtained [94–96].
- Deterministic spectral and spatial matching is not possible. Various tuning techniques can be used, such as temperature tuning, DC Stark shift tuning [97], and strain-tuning [94, 95].

To date, the research collaboration between UCSB (USA) and the Leiden University has been at the forefront in using this system as a platform for cavity QED, and we will briefly review several research highlights prior to the work presented in this thesis. Oxide apertured MPs are originally developed for vertical cavity laser applications (for example in the Larry Coldren group at UCSB), but were further developed to form high-quality factor microcavities by Stoltz *et al.* in 2005 [98]. In 2007, Strauf *et al.* developed a high-frequency single-photon source by embedding QDs in the cavity and implementing electrical gates [99]. The great potential for externally mode-matched cavity QED experiments with charge-controlled QDs was further demonstrated by Rakher *et al.* in 2009 [100]. Following this, techniques were developed to tune the cavity birefringence and at the same time tune QD transitions (Bonato *et al.*, 2009 [94], 2011 [95]) by applying laser induced surface defects.

Of the remaining challenges, two are addressed in this thesis and are to more reliably control the sample fabrication process, especially to fabricate the oxide aperture, and to further explore resonant spectroscopy of neutral and charged quantum dots coupled to a polarization degenerate microcavity in the intermediate coupling regime. Some of the remaining challenges, especially towards deterministic spin-photon entanglement, will be discussed in the final outlook Chapter.

1.6 Overview of this thesis

This thesis is organized in four sections: (i) an introductory section that provide a general overview of cavity QED (Chapter 1) and a more technical introduction to the setup, techniques and sample (Chapter 2), (ii) a section (Chapter 3-5) that is devoted to optimizing the oxide aperture, (iii) a section

(Chapter 6-8) on low-temperature cavity QED experiments, (iv) and finally an outlook (Chapter 9).

- In Chapter 2 we first introduce the magneto-optical cryostat setup, briefly explain the applied experimental techniques, the sample structure, and demonstrate quantum dot and sample characterization.

- In Chapter 3-5 we show our work on optimizing the oxide aperture; these chapters have a more engineering character. In Chapter 3 we first introduce a technique to monitor the formation of the oxide aperture in real time, as well as an efficient technique to characterize the samples at room temperature. These techniques are based on off-resonant and resonant reflectivity scans, respectively. For this purpose we developed a novel steam-oxidation furnace integrated with an optical viewport. In Chapter 4 we used the same setup and performed many successive oxidation steps on the same microcavity. We characterize the optical modes at room temperature after each oxidation step and demonstrate that this offers a precise technique to fine-tune the exact amount of oxidation and thereby the cavity mode properties. In Chapter 5 we show that by systematic variations of the size and shape of elliptical oxide apertures the polarization properties of the cavity modes can be controlled, and with this method polarization degenerate microcavities can be produced nearly deterministically.

- In Chapter 6-8 low-temperature cavity QED measurements with QDs coupled to a polarization degenerate microcavity are presented. In Chapter 6 we study both a neutral and a singly–charged QD through resonant reflection and transmission spectroscopy. We demonstrate a polarization resolved analysis that reveals coherent and incoherent dynamics, and introduce models that describe the various findings. In Chapter 7 we study a novel non-linear effect due to the cavity-enhanced feedback between a QD and a charge memory. At the origin lies the excitation of charges by the intracavity field, which are then trapped by the oxide aperture and which cause a blueshift of the QD. We then demonstrate how the cavity can be used as an accurate probe of the $\sim$ms timescale build-up and decay of these charges. In Chapter 8 we present a homodyne detection technique that enables to determine directly the coherence and phase of light that passes through a coupled QD-cavity system. We use this technique as a powerful tool to characterize coherent and incoherent QDs, to study quantum optics textbook physics of the coherent fraction

as function of laser intensity, and to demonstrate a quantum dot induced phase shift.

- In Chapter 9 we conclude with an outlook. During the time of this thesis an unique set of samples was developed with which many more experiments were explored. Furthermore, we will discuss some approaches to further develop coherent charged QDs that can be used for deterministic spin–photon entanglement.